Recognition determinants of broad and potent HIV-1 neutralization by an affinity matured antibody from a pediatric elite-neutralizer

Sanjeev Kumar[1,2,†], Swarandeep Singh[1,†], Arnab Chatterjee[3,†], Prashant Bajpai[2], Shaifali Sharma[1], Sanket Katpara[1], Rakesh Lodha[4], Somnath Dutta[3,*], Kalpana Luthra[1,*]

[1]Department of Biochemistry, All India Institute of Medical Sciences, New Delhi, India
[2]ICGEB-Emory Vaccine Center, International Center for Genetic Engineering and Biotechnology, New Delhi, India
[3]Molecular Biophysics Unit, Indian Institute of Science, Bangalore, India
[4]Department of Pediatrics, All India Institute of Medical Sciences, New Delhi, India

[†]Equal contribution

[*]**Correspondence**

E-mail: kalpanaluthra@gmail.com, somnath@iisc.ac.in

Keywords

HIV-1, clade-C, N332 supersite, pediatric HIV-1 bnAb, elite-neutralizer, SOSIP trimer, Cryo-EM structure

ABSTRACT

The structural and characteristic features of HIV-1 broadly neutralizing antibodies (bnAbs) from chronically infected pediatric donors are currently unknown. Herein, we characterized a heavy chain matured HIV-1 bnAb 44m, identified from a pediatric elite-neutralizer. Interestingly, in comparison to its wild-type AIIMS-P01 bnAb, 44m exhibited moderately higher level of somatic hypermutations (SHM) of 15.2%. 44m neutralized 79% of HIV-1 heterologous viruses tested, with a geometric mean IC_{50} titer of 0.36 µg/ml. The cryoEM structure of 44m Fab in complex with fully-cleaved glycosylated native-like BG505.SOSIP envelope trimer at 4.4 Å resolution revealed that 44m targets the V3-glycan N332-supersite and GDIR motif to neutralize HIV-1 with improved potency and breadth, plausibly attributed by a matured heavy chain as compared to that of wild-type AIIMS-P01 bnAb. This study improves our understanding on pediatric HIV-1 bnAbs and

structural basis of broad HIV-1 neutralization by 44m may be useful blueprint for vaccine design in future.

INTRODUCTION

Extensive efforts are currently ongoing worldwide to develop a safe and effective vaccine to human immunodeficiency virus-1 (HIV-1). During HIV-1 infection, neutralizing antibodies (nAbs) are elicited against the envelope (env) glycoprotein gp160[1,2]. Highly potent broadly neutralizing antibodies (bnAbs) are found to develop and evolve in only top 1% of HIV-1 infected individuals, classified as elite-neutralizers[3,4]. So far, seven distinct epitopes of HIV-1 bnAbs have been identified to be present on the viral env that are: V2-apex, V3-glycan N332-supersite, CD4 binding site (CD4bs), silent-face center (SFC), membrane-proximal external region (MPER), gp120–gp41 interface and fusion peptide (FP)[1]. Presently, the prime goal is to design and develop an HIV-1 vaccine capable of triggering naïve B cells and steer them to evolve into bnAb generating B cells upon immunization/vaccination[5–7].

HIV-1 infected infants have been shown to develop bnAb responses within one year of age[8,9]; while in infected adults, it takes at least 2 to 3 years post infection for the development of bnAbs[3,10,11], suggesting distinct maturation pathways of the bnAbs evolving in children[8,12]. The HIV-1 bnAbs isolated from adults have been extensively characterized, both structurally and functionally; with some of them exhibiting characteristic features of high somatic-hypermutations (SHM) and long CDR3 regions[1], while there is a paucity of such information on the bnAbs generated by HIV-1 infected children. A number of studies carried out on HIV-1 infected pediatric cohorts have reported HIV-1 plasma bnAb responses targeted at multiple env epitopes including the V2-apex, N332-glycan supersite, CD4bs and MPER[8,9,13–17]; however isolation of only two pediatric HIV-1 bnAbs have been reported thus far: BF520.1 by Simonich et al[9] and AIIMS-P01 by us[18]. Binding of both AIIMS-P01 and BF520.1 are dependent on the N332-supersite epitope present at the base of the V3-glycan region[9,18]. Both pediatric bnAbs exhibit limited SHM (~7%); however, there is paucity of information towards understanding whether an increased SHM can be acquired in bnAbs evolving in HIV-1 infected children and further, if the increased SHM in pediatric bnAbs can lead to increase

in their potency and breadth of viral neutralization, as observed in bnAbs evolving in HIV-1 infected adults[1,2,19–28].

Immunogenetic information of HIV-1 bnAbs from adults and children obtained from deep sequencing or single cell analysis of B cell repertoire (BCR) can further our understanding of their natural development during the course of infection and development of blueprints for rational vaccine design and effective vaccination strategies[5,6]. Furthermore, structural characterization of potent bnAbs, in complex with native-like trimeric env can provide useful mechanistic insights for broad and potent neutralization of HIV-1 heterologous viruses.

We previously reported the isolation of a bnAb AIIMS-P01, from an antiretroviral naïve HIV-1 clade-C chronically infected pediatric elite-neutralizer AIIMS_330[15,16,18,29,30]. Herein, to delineate the characteristics of an affinity matured lineage member antibody of the AIIMS-P01 pediatric bnAb, we performed the structural and functional characterization of a heavy chain matured pediatric HIV-1 AIIMS-P01 bnAb lineage monoclonal antibody clone 44m (referred to as 44m). The 44m exhibited moderate level of SHM (15.2%) and demonstrated near about 80% HIV-1 neutralization breadth with ~2 times improved potency than AIIMS-P01 wild-type (WT) bnAb. CryoEM analysis of 44m in complex with BG505.SOSIP trimer revealed structural insights for broad HIV-1 neutralization.

RESULTS

Identification of a matured AIIMS-P01 lineage antibody

We previously reported the isolation and characterization of a broad and potent anti-HIV-1 bnAb AIIMS-P01 from an Indian clade-C infected pediatric elite-neutralizer AIIMS_330[18]. To understand the role of affinity matured AIIMS-P01 antibody in HIV-1 neutralization, we performed the deep sequencing of bulk B cell repertoire from total peripheral blood mononuclear cells (PBMCs) of the AIIMS_330 pediatric elite-neutralizer (Kumar S et. al. unpublished data). We identified 21 heavy chain sequences that matched the CDRH3 sequence of AIIMS-P01, with varied and moderate level (30 nt – 47 nt) of antibody somatic hypermutations (SHM) (**Fig. S1**). We did not find matched CDRL3 light chain genes as that of the AIIMS-P01. As observed by us previously, the heavy chain

dominantly contributed to HIV-1 neutralization breadth[18]. Therefore, to understand the effect of higher level of SHM in matured AIIMS-P01 lineage members, herein, we synthesized a matured (15.2% SHM) AIIMS-P01 bnAb heavy chain gene with >85% similar CDRH3 sequence as of AIIMS-P01, designated as 44m and expressed the mAb by co-transfecting plasmids carrying this heavy chain gene and the WT AIIMS-P01 light chain gene.

Matured AIIMS-P01 lineage antibody 44m showed improved breadth and potency than AIIMS-P01

We first determined the binding reactivity of the matured 44m monoclonal antibody to heterologous HIV-1 monomeric and trimeric envelope proteins and observed high binding efficiency (**Fig. 1a**). To further validate the binding data obtained by ELISA, affinity analysis of the 44m with HIV-1 SOSIP trimer was performed using Octet BLI assays. Antibody 44m showed high nanomolar (nM) affinity (KD: 0.56 nM) with BG505.SOSIP.664 T332N (**Fig. 1b**). The neutralization potential of 44m mAb was tested against heterologous viruses and the global panel of HIV-1 viruses, at concentrations ranging from 10µg/ml to 0.001 µg/ml, using a TZM-bl based neutralization assay[31]. The 44m bnAb neutralized 77% HIV-1 clade-C viruses and 80% clade-B viruses and demonstrated an overall improvement of breadth of 79% against the heterologous viruses tested, and potency, with a geometric mean IC_{50} titer of 0.36 µg/ml, as compared to that of AIIMS-P01. Further, a 58% breadth, with IC_{50} titer of 0.43 µg/ml was observed, on testing this bnAb against the global panel of viruses (**Fig. 2**). The neutralizing activity data reveal an increase in potency and breadth of the matured version 44m against the heterologous viruses tested and increased SHM in comparison to AIIMS-P01 WT (**Fig. 1c, d**). These findings encouraged us to perform structural characterization of 44m antibody with the stabilized envelope BG505.SOSIP.664 T332N.

44m targets the V3 loop of Env and showed binding dependence on the GDIR Motif

Structural insight into mature 44m bnAb binding in the context of BG505.SOSIP a natively glycosylated Env was achieved by Cryo-Electron microscopy. The 44m bnAb Fab and BG505.SOSIP Env trimer were expressed and purified from Expi293F cells which include similar glycoforms as Env trimers expressed in human cells. We solved the structure with a global resolution of 4.4 Å and local resolution of 3.36 Å and 3.74 Å (**Fig. 3 and S2 – S5)**.

The atomic model fitted in the EM map of BG505 trimer in complex with Fab of the 44m bnAb displayed a total of three 44m Fabs, with one Fab bound to each protomer of the Env trimer for effective neutralization (**Fig. 3**). Cryo-EM structures of BG505.SOSIP Env trimer with 44m bnAb indicated trimeric shapes of HIV trimer, which additionally connected with extra densities, attributed to the corresponding bound Fab moieties (**Fig. S2b**). Different subdomains, gp120, gp41 and Fab densities were visible in the high-resolution cryo-EM structure of the Env trimer in complex with 44m bnAb (**Fig. 3**).

Structural analysis revealed that the CDRH3 loop of neutralizing antibody 44m stretched deep inside the groove between the N295 and N332 residues, thus reaching the base of the V3 loop of gp120 and established a range of chemical bonds with the nearby favorable amino acids (**Fig. 4a**). The total occupied surface area of 44m is ~750 $Å^2$, with extensive participation of the heavy chain. This surface area includes all the CDR regions and FR3 region, but the CDRH1 and CDRH3 loop show a predomination contribution. The positioning of the CDR regions of the heavy chain is crucial to establish contact points with the V3 loop of the gp120 **(Fig. 4a, b).** The key residues on the CDRH3 loop that are interacting with the gp120 region are V106, P107, A 108, R109, and W110, whereas the primary contact points of CDRH1 and CDRH2 loops with the CD4bs are H31, Y52, Y53, T54, D56, and T57 **(Fig. 4b)**. These interactions are mainly stabilized by both hydrogen bonding and van der Waals interactions. Interestingly, the R109 residue of the CDRH3 demonstrated a salt bridge interaction with the D325 site of the gp120 region **(Fig. 4c)**. These interacting residues are hidden within the different clefts of the V3 loop of the gp120 region. The surface potential map of the paratope region depicts the interacting residues of CDR regions placed near the polar residues of the V3 loop **(Fig. 4d and S6)**.

44m interacts with N332-supersite

The antibody-Env protein interaction studies unraveled the possibilities to explore the glycan antibody interactions. The atomic model demonstrated that the interaction sites for 44m bnAbs on gp120 were positioned in an area that is surrounded by three N-glycan patches: the Asn301, Asn332 located near the base of V3, the Asn156 glycan in the V1V2 region, and the Asn295 glycan near the bottom of gp120 **(Fig. 5a-d)**. This binding approach created an interlocked system of V_H loop of 44m and V3 loops of gp120, and forming a stable antibody-antigen complex **(Fig. 5b).** Glycan binding to N301 is forming

contacts with polar and charged amino acids of the CDRH2 loop, wherein the T54 and D56 of the CDRH2 region are interacting with the polar side of glycan moieties to mask the binding to host cells **(Fig. 5c)**. The N332 glycan engages in forming the largest interacting area, with most of the CDRH3 region involving different portions of glycan moieties on it. N-Acetyl glucosamine attached to the N332 residue is forming hydrogen bonding with Ser111 and Tyr113 residues of the CDRH3 region **(Fig. 5d).** The structural analysis showed that the 44m antibody interacts with different glycan moieties attached to asparagine residues at 301 and 332 positions in the V3 region.

44m showed distinct glycan binding interactions, with similar pattern of epitope interaction like other V3-glycan bnAbs

A comparative structural analysis of the 44m antibody with other available bnAbs (BG18, 10-1074, DH270.6 & BF520.1) was performed to understand the exceptionality of this 44m antibody **(Fig. S6 - S8)**. Superimposition of the antibodies directed at the V3 loop region of the gp120 protomer showed a common interaction pattern across all the bnAbs within the V3 region. In the BG18 bnAb (6dfg) CDRL3 and CDRH3 loops are interacting with V3 region for stalking of the antibody onto the gp120 (**Fig. S8a**). In bnAb 10-1074 (6udj), the V3 loop of gp120 protomer interacts with CDRH3 and CDRL3 regions (**Fig. S8b**). DH270.6 (6um6) and BF520.1 (6mn7) have more inter-facial area**,** which helps in the interaction of residues in CDRL1 and CDRL2 regions. Additionally, the V1 region interacts with the CDRL3 loop (**Fig. S8c, d**). The V3 loop has stable bonding with the CDRH1 loop for effective neutralization. The presence of an 8 amino acid long elongated face in the CDRH3 region in PGT121 and PGT122 classes of antibodies make these antibodies potent to bind gp120 surface using two functional surfaces (**Fig. S8e**). These results suggest that the overall binding region of the CDR with both V3 and V1/V2 loops were significantly increased. The superimposition of V3-glycan bnAbs into the gp120 trimer depicts the variability in the binding surface area but a common binding pattern on the gp120.

44m HIV-1 bnAb showed co-dependence on GDIR motif and N332-supersite

Results obtained from structural mapping of 44m showed that this bnAb binds the N156, N295, N301, D325 residue of GDIR motif and N332-supersite env regions **(Fig. 3c & 4b)**. Next, we used this structural mapping information to understand the linkage of these

residues in 44m mediated HIV-1 neutralization by performing sequence alignment of these identified contact residues within the envelope regions of the viruses tested. The analysis revealed that the N156 and N301 glycans are relatively conserved whereas mutations at the N295 residue are present heterogeneously among the 44m resistant and susceptible viruses, suggesting these mutations may not be majorly contributing to the 44m mediated viral neutralization (**Fig. S9**). In contrast, mutations present at D325 and N332 positions were found to be associated with abrogation in neutralization potential of 44m and vice-versa, e.g. HXB2, ZM249 and ZM233 viruses were resistant to neutralization by 44m, due to the absence of GDIR epitope in these viruses. These findings suggest that the neutralization dependence of the pediatric bnAb 44m relies on the D325 residue of GDIR motif and N332-spersite, as has also been reported for the adult HIV-1 V3 bnAbs PGT121 and 10-1074.

DISCUSSION

The footprints of HIV-1 broadly neutralizing antibodies (bnAbs) can provide a template for structure-guided vaccine design[5,6]. Highly potent bnAb based therapeutics, prophylactics and vaccines are attractive strategies to tackle HIV-1[1]. Immunogenetics based information of potent HIV-1 bnAbs derived from deep sequencing or single cell analysis of B cell repertoire (BCR) of infected donors can provide critical insights towards understanding their natural development during the course of infection and reveal the frequency of B cells within the human B cell repertoire, that can elicit potent bnAbs to guide vaccination strategies[5,25,32,33]. Further, the structural characterization of potent HIV-1 bnAbs in complex with the viral envelope provides useful mechanistic insights of viral neutralization and information of epitope-paratope interaction for rational vaccine design[6]. Currently, the leading strategy in innovative HIV-1 next-generation immunotherapeutic and vaccine design is to develop and elicit bnAb responses by steering bnAb expressing B cells[5,7]. To achieve this goal, it is essential to understand the structural mechanism of HIV-1 neutralization and immunogenetics of B cells that elicit potent bnAbs. The evolution of HIV-1 bnAbs from adult donors has been studied extensively[25,34,35], but, no information is available on the evolving HIV-1 bnAb lineage in chronically infected children.

Herein, to fill this knowledge gap, we synthesized a heavy chain matured lineage member of AIIMS-P01 bnAb and evaluated its structural features and functionality in terms of viral binding and neutralization activity. We used only heavy chain of AIIMS-P01 matured lineages as we didn't find matched CDRL3 of the AIIMS-P01 light chain in our deep sequencing data (unpublished), plausibly due to the low depth of sequencing. We combined functional and structural approaches and showed that maturation in the 44m heavy chain, like that reported for the adult bnAbs of the PGT class[34,36], was functionally important for HIV-1 Env binding and neutralization. This was demonstrated by the increased heterologous breadth observed when the mature heavy chain was paired with the original light chain of AIIMS-P01 WT bnAb, suggesting that the recently acquired SHMs can be functionally important for the evolution and neutralization breadth for this bnAb. In addition, the matured bnAb 44m exhibited a change of indel sequence (SNPSR mutated to SDPIR**,** in comparison to its WT bnAb AIIMS-P01 **(Fig. 4e)**, specifically from non-polar residues to acidic & hydrophobic residues, which plausibly creates an electronegativity that could enhance the contact of antibody loops with the virus.

Unlike HIV-1 CD4bs bnAbs, the V3-glycan targeting bnAbs are of high interest because they are common and not restricted by certain germline genes[1,2]. The pediatric bnAb AIIMS-P01 and infant derived BF520.1 are of particular interest because these showed broad HIV-1 neutralization despite limited SHM[9,18]. The 44m lineage bnAb identified and characterized herein showed improved neutralization potency and breadth plausibly by acquisition of higher number of SHM, that led to an increase in potency twice that of the WT AIIMS-P01 bnAb. The Cryo-EM structural analysis of bnAb 44m, indicated that CDRH1 (H31, Y53 and T57) and CDRH3 (P107, A108 and R109) residues appear to contribute to the 44m paratope by mediating contacts with the conserved V3-glycan N332-supersite, D325 of 'GDIR' sequence motif, glycans at position 137, 156, 295, 301 and 332. These major determinants of neutralization breadth interacting with residues within the CDRH1 and CDRH3 regions of the 44m, similar to that in the adult bnAbs and distinct from the infant bnAb BF520.1[9,34]. The angle of approach by 44m towards the V3 epitope was previously determined to be similar to PGT121[37,38], although the positioning of 44m was notably different and slightly rotated relative to the PGT121. The crystal structure of PGT121 in complex with gp120 identified the GDIR motif and glycans at positions N332 and N301 as the primary contacts defining the PGT121 epitope[37,38]. The

CDRH3 loop, which is highly mutated in PGT121, penetrates the glycan shield in order to contact both the GDIR motif and N332 glycan.

The structural model similarly indicates potential CDRH3 contacts with the GDIR motif and N332 glycan. However, structurally defined epitope-paratope interface do not fully capture the functional binding contacts that drive neutralization and escape[39], reinforcing the gravity of functional assays to define the recognition determinants that are important for neutralization activity. Though we observed that 44m interacts with other V3-region glycans including N295 and N301, however, HIV-1 viral sequence alignment revealed that 44m is primarily dependent on N332-glycan supersite and GDIR motifs. Based on the findings of HIV-1 binding, neutralization and structural analysis of the 44m pediatric bnAb, we postulate that a germline targeting vaccine / immunogen could easily elicit AIIMS-P01 / 44m-like responses. In the AIIMS_330 pediatric elite neutralizer, the circulating and coevolving viruses may have led to elicitation of this bnAb lineage (44m), to drive affinity maturation in the AIIMS-P01 bnAb, as has been observed previously for the evolution of V1V2 and V3-glycan plasma bnAbs[15].

In summary, the structural and functional characterization of a heavy chain matured pediatric bnAb 44m showed improved HIV-1 neutralization potency and breadth in comparison to its WT bnAb AIIMS-P01. This study for the first time provides an evidence towards contribution of antibody SHM in improved HIV-1 neutralizing efficiency of a pediatric bnAb. Further studies in this direction are required to be conducted to understand the antigenic triggers in chronically infected children that can elicit similar protective bnAbs targeting other HIV-1 bnAb epitopes which in turn can provide simpler blueprint to guide HIV-1 vaccine design.

METHODS

Ethics statement

This study was conducted after obtaining approval from the institutional ethics committee, All India Institute of Medical Sciences (AIIMS), New Delhi, India (IEC/-532/1111.2016 & IEC-72/01.02.2019).

Antibody gene synthesis

The antibody heavy chain genes of matured AIIMS-P01 lineage antibody was synthesized after codon-optimization for mammalian expression from Genscript, Inc. USA, and cloned in respective monoclonal antibody expression vector AbVec under AgeI and SalI sites[40].

Antibody genes sequence analysis

The sequencing of the antibody genes was done commercially from Eurofins, India. The sequences were analyzed online through IMGT/V-QUEST (http://www.imgt.org/IMGT_vquest/vquest)[41].

Expression of monoclonal antibodies

All HIV-1 mAbs were expressed in Expi293F cells (Thermo Fisher) as described previously[18,42]. Briefly, 15µg each of heavy chain and light chain expressing IgG1 plasmids were co-transfected using PEI-Max as transfection reagent. Following 4-6 days of incubation, cells were harvested by centrifugation and filtered through 0.22 mm syringe filter (mdi). The supernatant was added to a Protein A column affinity chromatography column (Pierce). The column was then washed with 1×PBS and mAbs were eluted with IgG Elution Buffer (Pierce), immediately neutralized with 1M Tris pH 8.0 buffer and extensively dialyzed against 1×PBS at 4°C. The mAbs were then concentrated using 10kDa Amicon Ultra-15 centrifugal filter units (EMD Millipore), filtered through a 0.22 mm syringe filter (mdi) and stored at -80°C for further use.

Expression and purification of BG505.SOSIP.664 T332N trimeric proteins

The BG505.SOSIP.664.C2 T332N gp140 trimeric proteins with twin-strep-tag was expressed in HEK 293F cells and purified by methods described previously[36,43]. Purity was assessed by blue native polyacrylamide gel electrophoresis (BN-PAGE) and binding reactivity with HIV-1 bnAbs was assessed by ELISA.

Binding analysis of mAbs by ELISA

Briefly, 96-well ELISA plates (Costar) were coated with 5µg/ml recombinant HIV-1 gp120 monomeric proteins overnight at 4°C in 0.1 M $NaHCO_3$ (pH 9.6). Next day, plates were washed thrice with 1×PBS (phosphate buffered saline) and blocked with 15% FBS RPMI and 2% BSA. After 1.5 hours of blocking at 37°C, plates were washed thrice with 1×PBS.

Then, serial dilutions of monoclonal antibodies (mAbs) were added and incubated for 1 hour at 37°C. Next, alkaline phosphatase (AP) labelled anti-Fc secondary antibody (Southern Biotech) at 1:2,000 was added and plates were incubated at 37°C for 1 hour. Plates were then washed thrice with 1×PBS and AP substrate tablets (Sigma) dissolved in diethanolamine (DAE) was added and incubated for 30 min at room temperature in the dark and readout was taken at 405nm. The BG505.SOSIP.664 gp140 trimeric ELISA was performed as described previously[43].

HIV-1 pseudovirus generation

The HIV-1 pseudoviruses were produced in HEK 293T cells as described earlier[15,18] by co-transfecting the full HIV-1 gp160 envelope plasmid and a pSG3ΔEnv backbone plasmid. Briefly, 1×10^5 cells in 2ml complete DMEM (10% fetal bovine serum (FBS) and 1% penicillin and streptomycin antibiotics) were seeded per well of a 6 well cell culture plate (Costar) the day prior to co-transfection for HIV-1 pseudovirus generation. For transfection, envelope (1.25µg) to delta envelope plasmid (2.50µg) ratio was 1:2, this complex was made in Opti-MEM (Gibco) with a final volume of 200µl for each well of the 6 well plate and incubated for 5 minutes at room temperature. Next, 3µl of PEI-Max transfection reagent (Polysciences) (1mg/ml) was added to this mixture, mixed well and further incubated for 15 min at room temperature. This mixture was then added dropwise to HEK 293T cells supplemented with fresh complete DMEM growth media and incubated at 37°C for 48 hours. Pseudoviruses were then harvested by filtering cell supernatants with 0.45 mm sterile filter (mdi) and stored frozen at −80°C as aliquots.

HIV-1 neutralization assays

The HIV-1 neutralization assays of monoclonal antibodies (mAbs) were done as described earlier[31,44]. Neutralization was measured as a reduction in luciferase gene expression after a single round of infection of TZM-bl cells (NIH AIDS Reagent Program) with HIV-1 envelope pseudoviruses. The $TCID_{50}$ of the HIV-1 pseudoviruses was calculated and 200 $TCID_{50}$ of the virus was used in neutralization assays by incubating with 1:3 serially diluted mAbs starting at 10 µg/ml. After that, freshly trypsinized TZM-bl cells in growth medium (complete DMEM with 10% FBS and 1% penicillin and streptomycin antibiotics) containing 50µg/ml DEAE Dextran and 1 mM Indinavir (in case of primary isolates) at 10^5 cells/well were added and plates were incubated at 37°C for

48 hours. Virus controls (cells with HIV-1 virus only) and cell controls (cells without virus and antibody) were included. MuLV was used as a negative control. After the incubation of the plates for 48 hours, luciferase activity was measured using the Bright-Glow Luciferase Assay System (Promega). IC_{50} for antibodies were calculated. Values were derived from a dose-response curve fit with a non-linear function using the GraphPad Prism 9 software (San Diego, CA).

Fab Fragment Preparation

The Fab fragments were generated from 4 mg of 44m IgG antibody using a Fab Fragmentation Kit (G Biosciences) according to manufacturer's protocol. Purity and size of Fab fragments were assessed by SDS-PAGE.

Octet BLI analysis

Octet biolayer interferometry (BLI) was performed using an Octet Red96 instrument (ForteBio, Inc.). A 5 µg/ml concentration of each mAb was captured on a protein A sensor and its binding kinetics were tested with serial 2-fold diluted HIV-1 SOSIP trimer protein (100 nM to 6.25 nM). The baseline was obtained by measurements taken for 60 s in BLI buffer (1x PBS and 0.05% Tween-20), and then, the sensors were subjected to association phase immersion for 300 s in wells containing serial dilutions of HIV-1 SOSIP protein. Then, the sensors were immersed in BLI buffer for as long as 600 s to measure the dissociation phase. The mean Kon, Koff and apparent KD values of the mAbs binding affinities for HIV-1 SOSIP envelope protein were calculated from all the binding curves based on their global fit to a 1:1 Langmuir binding model using Octet software version 12.0.

Negative-stain EM

To observe the binding pattern of 44m bnAb to BG505 SOSIP trimer and the homogeneity of the complex, we first performed room temperature negative staining TEM. The SEC purified complex of BG505 SOSIP trimer and 44m bnAb (1.2 mg/ml) was diluted by 70 times for analysis. The 3.5 µl of sample mixture was put onto a glow discharged carbon coated Cu grids for 30 secs (EM grid, 300 mesh, Electron Microscopy Sciences). After 1.5 min of incubation of the sample on the grid, the remained solvent was blotted and three

drops of 1% uranyl acetate (Uranyl Acetate 98%, ACS Reagent, Polysciences, Inc.) was applied on the grid for staining purpose. The excess stain was blotted after each addition and after air dried, the grid was used for data collection with 120 kV Talos L120C electron microscope. Data acquisition was performed using 4k x 4k Ceta camera at the magnification of 73kx and it is calibrated at 3.84Å/pixel. The collected images were processed in EMAN 2.1[45]. From these micrographs we picked particles in both manual and automated mode, and its co-ordinates were extracted using e2boxer.py in EMAN 2.1. Followed by, reference free 2D class averages were performed to analyze different views of bnAb bound trimer complex. The cleaned particles after extraction were taken for reference-free 2D class averages using simple_prime2D of SIMPLE 2.1 software[46] with a mask diameter of 30 pixels at 3.84 Å/pix.

Sample preparation for cryoEM

R1.2/1.3 300 mesh copper grids (Quantifoil) (Electron Microscopy Sciences) were glow discharged at 20mA for 90 seconds before cryo-freezing. Three microliters of the SEC purified complex of BG505 SOSIP trimer and 44m bnAb (1.2 mg/ml) was applied onto the freshly glow discharged grid, and immediately blotted for 8.5 secs without any blot force just after 10 secs of incubation to remove excess solvent in pre-equilibrated chamber of FEI Vitrobot Mark IV plunger. The sample was plunged into the liquid ethane just after blotting.

CryoEM data acquisition

Cryo-EM data were collected using 200 kV TalosArctica transmission electron microscope (Thermo Scientific™) equipped with Gatan K2 Summit Direct Electron Detector. Movies were recorded automatically using Latitude-S (DigitalMicrograph - GMS 3.5) at nominal magnification of 45,000x at the effective pixel size of 1.17 Å (*14*). Micrographs were acquired in counting mode with a total dose of 60 e^-/Å2, with an exposure time of 8 sec distributed for 20 frames. A total of 3000 movies were acquired for the BG505 SOSIP trimer and 44m bnAbs protein complexes respectively.

CryoEM data analysis and model building

Single-Particle Analysis (SPA) were performed for the acquired cryo-EM movies using the Relion version 3.1[47]. At first, drift and gain corrections of the individual movies were

performed with MotionCorr2[48]and estimated Contrast transfer function (CTF) parameters using CTFFIND 4.1.13[49]. Subsequently, CTF estimated micrographs were subjected to analyze to eliminate bad micrographs using cisTEM[50] and also, to remove poor resolution micrographs with a fit resolution threshold of 7 Å. The particles from best micrographs were chosen for automated picking using 2D reference in Relion and extracted with the box sizes of 280 Å for the BG505 SOSIP trimer and 44m bnAb complexes. After three rounds of rigorous 2D classification good classes with high-resolution features of the complex were obtained as 1080743 particles. These well-defined particles were selected for 3D classification with C3 symmetry. To achieve high resolution, all particles belonging to the best classes of the complex was accounted for 3D auto-refinement and followed by movie refinement. The sharpening for the 3D auto-refined maps was performed with Relion 3.1[47] and PHENIX[51]. Overviews of cryo-EM data processing is shown in **Table S2**. Global resolution of Fourier shell correlation (FSC) was estimated at the threshold of 0.143 and the estimation of local resolution were performed with ResMap, using two auto-refined half maps.

Automated model building was iteratively done with Phenix Real Space Refinement. Only the Env trimer (PDB ID: 5aco) was docked with cryo-EM maps using UCSF Chimera "Fit in map" tool. To build the model for bnAb, the query sequences of the Fab was submitted to Swiss-Model and the resultant model was also fitted in the EM maps. The structural statistics for Cryo-EM map and atomic model were analyzed using Phenix[51], EMringer[52], Molprobity[53], and UCSF chimera[54]. Cryo-EM map and atomic model were visualized using UCSF ChimeraX[55].

Quantification and statistical analysis

All statistical analysis was done with GraphPad Prism software version 9.

DATA AVAILABILITY

The sequence of the 44m heavy chain variable region has been deposited in GenBank with accession numbers xxx and xxx respectively. The PDB ID for the EM map of 44m Fab in complexed with BG505.SOSIP.664.C2 T332N gp140 trimer reported in this study is EMD: xxx PDB:xxx .Any additional data are available upon reasonable request from the corresponding authors. Source data are provided in this paper.

ACKNOWLEDGMENTS

This antibody work was supported by Department of Biotechnology, India Indo-SA grant (BT/PR2450/MED/29/1222/2017) and (BT/PR30120/MED/29/1339/2018) grants awarded to K.L. The cryoEM work and consumables were supported by DBT BUILDER PROGRAM (BT/INF/22/SP22/844/2107), DST-FIST (SR/FST/LSII-039/2015) and SERB (SERB-EMR/2016/000608, SERB-IPA/2020/000094) grants awarded to S.D. S.K. is supported through DBT/Wellcome Trust India Alliance Early Career Fellowship grant IA/E/18/1/504307 (S.K.). We are very much thankful to NIH AIDS reagent program for HIV-1 research reagents, Neutralizing antibody consortium (NAC), IAVI, USA for HIV-1 neutralizing antibodies.

AUTHOR CONTRIBUTIONS

Experimental work, data acquisition and analysis of data by S.Ku., S.D.S., A.C., P.B., S.S, S.Ka, R.L., S.D. Conceptualization and implementation by S.Ku., S.D.S., S.D. and K.L. Manuscript writing by S.Ku., S.D.S., A.C., S.D. and K.L. All authors reviewed the manuscript and approved the final version of the manuscript.

COMPETING INTERESTS

All the authors have read and approved the manuscript for publication and declare no competing interests.

REFERENCES

1. Sok, D. & Burton, D. R. Recent progress in broadly neutralizing antibodies to HIV. *Nat. Immunol.***19**, 1179–1188 (2018).
2. Burton, D. R. & Hangartner, L. Broadly Neutralizing Antibodies to HIV and Their Role in Vaccine Design. *Annu. Rev. Immunol.***34**, 635–659 (2016).
3. Euler, Z. & Schuitemaker, H. Cross-reactive broadly neutralizing antibodies: timing is everything. *Front. Immunol.***3**, 215 (2012).
4. Simek, M. D. *et al.* Human immunodeficiency virus type 1 elite neutralizers: individuals with broad and potent neutralizing activity identified by using a high-throughput neutralization assay together with an analytical selection algorithm. *J. Virol.***83**, 7337–7348 (2009).
5. Andrabi, R., Bhiman, J. N. & Burton, D. R. Strategies for a multi-stage neutralizing antibody-based HIV vaccine. *Curr. Opin. Immunol.***53**, 143–151 (2018).
6. Burton, D. R. What Are the Most Powerful Immunogen Design Vaccine Strategies? Reverse Vaccinology 2.0 Shows Great Promise. *Cold Spring Harb. Perspect. Biol.***9**, (2017).
7. del Moral-Sánchez, I. *et al.* High thermostability improves neutralizing antibody responses induced by native-like HIV-1 envelope trimers. *Npj Vaccines***7**, 1–12 (2022).
8. Goo, L., Chohan, V., Nduati, R. & Overbaugh, J. Early development of broadly neutralizing antibodies in HIV-1-infected infants. *Nat. Med.***20**, 655–658 (2014).
9. Simonich, C. A. *et al.* HIV-1 Neutralizing Antibodies with Limited Hypermutation from an Infant. *Cell***166**, 77–87 (2016).
10. Khan, L. *et al.* Identification of CD4-Binding Site Dependent Plasma Neutralizing Antibodies in an HIV-1 Infected Indian Individual. *PloS One***10**, e0125575 (2015).
11. Khan, L. *et al.* Cross-neutralizing anti-HIV-1 human single chain variable fragments(scFvs) against CD4 binding site and N332 glycan identified from a recombinant phage library. *Sci. Rep.***7**, 45163 (2017).
12. Fouda, G. G. *et al.* Immunological mechanisms of inducing HIV immunity in infants. *Vaccine***38**, 411–415 (2020).
13. Ditse, Z. *et al.* HIV-1 SUBTYPE C INFECTED CHILDREN WITH EXCEPTIONAL NEUTRALIZATION BREADTH EXHIBIT POLYCLONAL RESPONSES TARGETING KNOWN EPITOPES. *J. Virol.* (2018) doi:10.1128/JVI.00878-18.

14. Muenchhoff, M., Prendergast, A. J. & Goulder, P. J. R. Immunity to HIV in Early Life. *Front. Immunol.***5**, 391 (2014).
15. Mishra, N. *et al.* Viral characteristics associated with maintenance of elite neutralizing activity in chronically HIV-1 clade C infected monozygotic pediatric twins. *J. Virol.* JVI.00654-19 (2019) doi:10.1128/JVI.00654-19.
16. Makhdoomi, M. A. *et al.* Evolution of cross-neutralizing antibodies and mapping epitope specificity in plasma of chronic HIV-1-infected antiretroviral therapy-naïve children from India. *J. Gen. Virol.***98**, 1879–1891 (2017).
17. Mishra, N. *et al.* Broadly neutralizing plasma antibodies effective against autologous circulating viruses in infants with multivariant HIV-1 infection. *Nat. Commun.***11**, 4409 (2020).
18. Kumar, S. *et al.* An HIV-1 Broadly Neutralizing Antibody from a Clade C-Infected Pediatric Elite Neutralizer Potently Neutralizes the Contemporaneous and Autologous Evolving Viruses. *J. Virol.***93**, (2019).
19. Scheid, J. F. *et al.* Sequence and structural convergence of broad and potent HIV antibodies that mimic CD4 binding. *Science***333**, 1633–1637 (2011).
20. Freund, N. T. *et al.* Coexistence of potent HIV-1 broadly neutralizing antibodies and antibody-sensitive viruses in a viremic controller. *Sci. Transl. Med.***9**, (2017).
21. Walker, L. M. *et al.* Broad and potent neutralizing antibodies from an African donor reveal a new HIV-1 vaccine target. *Science***326**, 285–289 (2009).
22. Walker, L. M. *et al.* Broad neutralization coverage of HIV by multiple highly potent antibodies. *Nature***477**, 466–470 (2011).
23. Huang, J. *et al.* Broad and potent neutralization of HIV-1 by a gp41-specific human antibody. *Nature***491**, 406–412 (2012).
24. Huang, J. *et al.* Identification of a CD4-Binding-Site Antibody to HIV that Evolved Near-Pan Neutralization Breadth. *Immunity***45**, 1108–1121 (2016).
25. Bonsignori, M. *et al.* Staged induction of HIV-1 glycan-dependent broadly neutralizing antibodies. *Sci. Transl. Med.***9**, (2017).
26. Falkowska, E. *et al.* Broadly neutralizing HIV antibodies define a glycan-dependent epitope on the prefusion conformation of gp41 on cleaved envelope trimers. *Immunity***40**, 657–668 (2014).
27. Schoofs, T. *et al.* Broad and Potent Neutralizing Antibodies Recognize the Silent Face of the HIV Envelope. *Immunity***50**, 1513-1529.e9 (2019).

503 28. Doria-Rose, N. A. *et al.* New Member of the V1V2-Directed CAP256-VRC26 Lineage
504 That Shows Increased Breadth and Exceptional Potency. *J. Virol.***90**, 76–91 (2016).
505 29. Aggarwal, H. *et al.* Alterations in B Cell Compartment Correlate with Poor
506 Neutralization Response and Disease Progression in HIV-1 Infected Children. *Front.*
507 *Immunol.***8**, 1697 (2017).
508 30. Kumar, S. *et al.* CD4-Binding Site Directed Cross-Neutralizing scFv Monoclonals from
509 HIV-1 Subtype C Infected Indian Children. *Front. Immunol.***8**, 1568 (2017).
510 31. Montefiori, D. C. Measuring HIV neutralization in a luciferase reporter gene assay.
511 *Methods Mol. Biol. Clifton NJ***485**, 395–405 (2009).
512 32. Setliff, I. *et al.* Multi-Donor Longitudinal Antibody Repertoire Sequencing Reveals the
513 Existence of Public Antibody Clonotypes in HIV-1 Infection. *Cell Host Microbe***23**, 845-
514 854.e6 (2018).
515 33. Willis, J. R. *et al.* Human immunoglobulin repertoire analysis guides design of vaccine
516 priming immunogens targeting HIV V2-apex broadly neutralizing antibody
517 precursors. *Immunity***0**, (2022).
518 34. Sok, D. *et al.* The effects of somatic hypermutation on neutralization and binding in
519 the PGT121 family of broadly neutralizing HIV antibodies. *PLoS Pathog.***9**, e1003754
520 (2013).
521 35. Bonsignori, M. *et al.* Maturation Pathway from Germline to Broad HIV-1 Neutralizer
522 of a CD4-Mimic Antibody. *Cell***165**, 449–463 (2016).
523 36. Sok, D. *et al.* Recombinant HIV envelope trimer selects for quaternary-dependent
524 antibodies targeting the trimer apex. *Proc. Natl. Acad. Sci. U. S. A.***111**, 17624–17629
525 (2014).
526 37. Julien, J.-P. *et al.* Broadly neutralizing antibody PGT121 allosterically modulates CD4
527 binding via recognition of the HIV-1 gp120 V3 base and multiple surrounding glycans.
528 *PLoS Pathog.***9**, e1003342 (2013).
529 38. Mouquet, H. *et al.* Complex-type N-glycan recognition by potent broadly neutralizing
530 HIV antibodies. *Proc. Natl. Acad. Sci. U. S. A.***109**, E3268-3277 (2012).
531 39. Dingens, A. S., Arenz, D., Weight, H., Overbaugh, J. & Bloom, J. D. An Antigenic Atlas of
532 HIV-1 Escape from Broadly Neutralizing Antibodies Distinguishes Functional and
533 Structural Epitopes. *Immunity***50**, 520-532.e3 (2019).
534 40. Smith, K. *et al.* Rapid generation of fully human monoclonal antibodies specific to a
535 vaccinating antigen. *Nat. Protoc.***4**, 372–384 (2009).

41. Lefranc, M.-P. *et al.* IMGT, the international ImMunoGeneTics information system. *Nucleic Acids Res.***37**, D1006-1012 (2009).
42. Kumar, S. *et al.* Structural insights for neutralization of Omicron variants BA.1, BA.2, BA.4, and BA.5 by a broadly neutralizing SARS-CoV-2 antibody. *Sci. Adv.***8**, eadd2032 (2022).
43. Sanders, R. W. *et al.* A next-generation cleaved, soluble HIV-1 Env trimer, BG505 SOSIP.664 gp140, expresses multiple epitopes for broadly neutralizing but not non-neutralizing antibodies. *PLoS Pathog.***9**, e1003618 (2013).
44. Kumar, S. *et al.* Effect of combination antiretroviral therapy on human immunodeficiency virus 1 specific antibody responses in subtype-C infected children. *J. Gen. Virol.***101**, 1289–1299 (2020).
45. Bell, J. M., Chen, M., Baldwin, P. R. & Ludtke, S. J. High resolution single particle refinement in EMAN2.1. *Methods San Diego Calif***100**, 25–34 (2016).
46. Reboul, C. F., Eager, M., Elmlund, D. & Elmlund, H. Single-particle cryo-EM-Improved ab initio 3D reconstruction with SIMPLE/PRIME. *Protein Sci. Publ. Protein Soc.***27**, 51–61 (2018).
47. Scheres, S. H. W. RELION: Implementation of a Bayesian approach to cryo-EM structure determination. *J. Struct. Biol.***180**, 519–530 (2012).
48. Zheng, S. Q. *et al.* MotionCor2: anisotropic correction of beam-induced motion for improved cryo-electron microscopy. *Nat. Methods***14**, 331–332 (2017).
49. Rohou, A. & Grigorieff, N. CTFFIND4: Fast and accurate defocus estimation from electron micrographs. *J. Struct. Biol.***192**, 216–221 (2015).
50. Grant, T., Rohou, A. & Grigorieff, N. cisTEM, user-friendly software for single-particle image processing. *eLife***7**, e35383 (2018).
51. Adams, P. D. *et al.* PHENIX: a comprehensive Python-based system for macromolecular structure solution. *Acta Crystallogr. D Biol. Crystallogr.***66**, 213–221 (2010).
52. Barad, B. A. *et al.* EMRinger: side chain–directed model and map validation for 3D cryo-electron microscopy. *Nat. Methods***12**, 943–946 (2015).
53. Williams, C. J. *et al.* MolProbity: More and better reference data for improved all-atom structure validation. *Protein Sci. Publ. Protein Soc.***27**, 293–315 (2018).
54. Pettersen, E. F. *et al.* UCSF Chimera--a visualization system for exploratory research and analysis. *J. Comput. Chem.***25**, 1605–1612 (2004).

569 55. Goddard, T. D. *et al.* UCSF ChimeraX: Meeting modern challenges in visualization and
570 analysis. *Protein Sci. Publ. Protein Soc.***27**, 14–25 (2018).

571

FIGURES WITH FIGURE LEGENDS

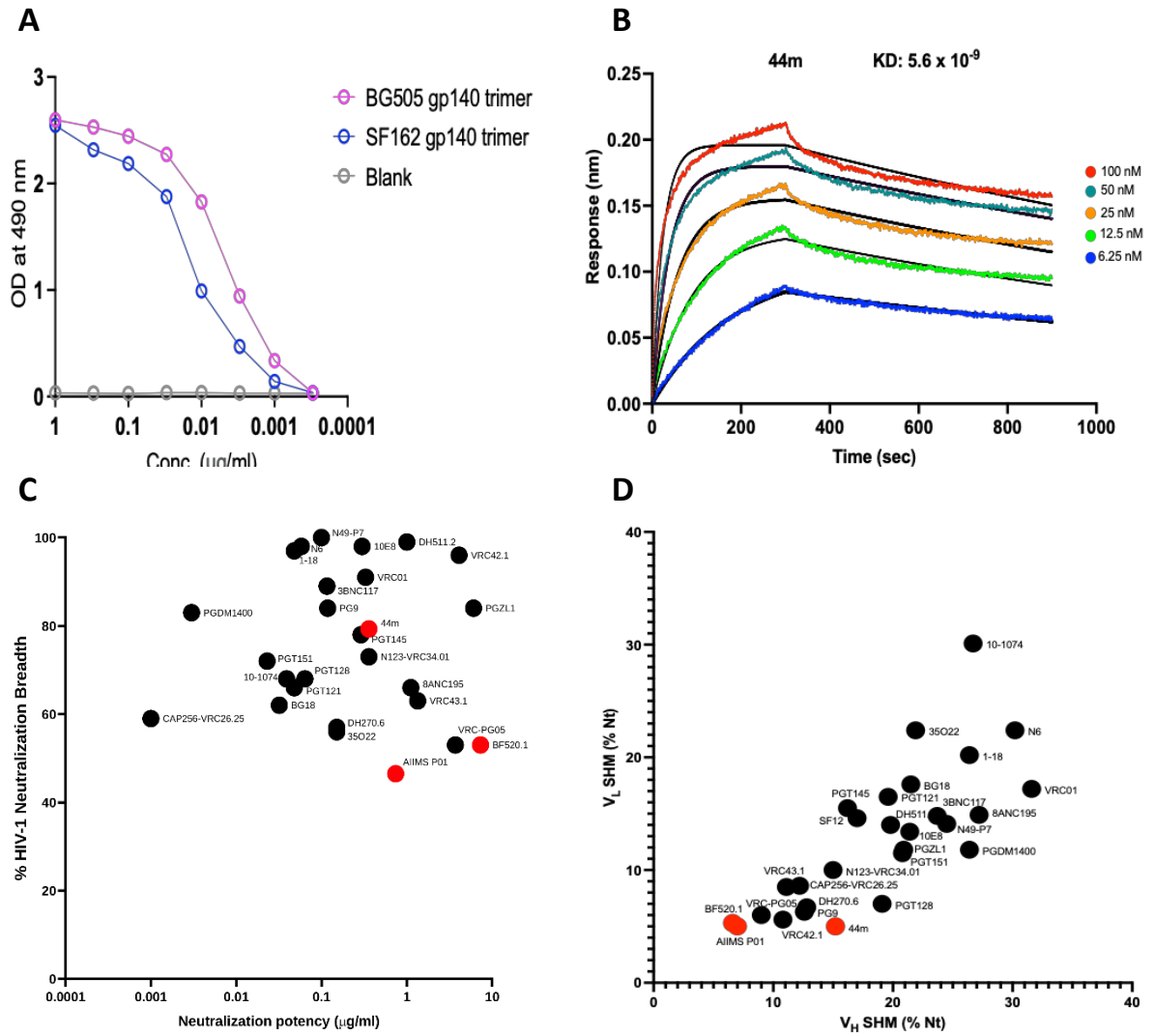

Figure 1: Binding Reactivity and Affinity of matured 44m bnAb to heterologous HIV-1 envelope glycoproteins. (A) Antigen Binding reactivity of the 44m mAb to heterologous HIV-1 trimeric envelope proteins determined by ELISA. **(B)** Binding Affinity of 44m to BG505 envelope trimer determined by Octet BLI. **(C)** Neutralization breadth comparison of HIV-1 adult and pediatric bnAbs is shown. **(D)** Somatic hypermutation (SHM) analysis of HIV-1 adult and pediatric bnAbs shown as % nucleotide (Nt) mutations relative to respective germline variable gene sequence. Here, pediatric HIV-1 bnAbs are highlighted in red color.

A

Global Panel					
S.No.	Virus ID	Tier	Clade	AIIMS_P01	AIIMS_P01_44
1	CNE55	3	AE	>10	>10
2	TRO11	2	B	1.5	1.15
3	CNE8	2	AE	>10	>10
4	CH119	2	BC	0.75	0.45
5	25710	1B	C	1.2	0.7
6	X2278	2	B	5.7	1.41
7	246F3	3	A/C	> 10	>10
8	X1632	2	G	>10	>10
9	CE1176	2	C	0.8	0.26
10	398F1	2	A	0.25	0.16
11	CEO217	3	C	>10	>10
12	BJOX 2000	2	BC	0.25	0.15
	GMT			0.87	0.43
	Breath			58%	58%

B

S.No.	Virus ID	Tier	Clade	AIIMS_P01	AIIMS_P01_44
1	QB726.70.M env C4	1B	A	>10	0.15
2	Q769.ENV H5	1B	A	>10	0.6
3	700010058.A4.4375	1B	B	2.5	0.35
4	SF162	1A	B	0.023	0.022
5	CAAN	2	B	1.55	0.1
6	WITO	2	B	>10	>10
7	TRJO	3	B	>10	>10
8	RHPA	2	B	4.1	0.5
9	TR011	2	B	3	0.2
10	AC10	2	B	>10	0.65
11	QHO692	2	B	>10	2.7
12	SC422661.8	2	B	4.65	0.95
13	1012.TC21.3257	1B	B	>10	0.6
14	1059_09.A4.1460	2	B	>10	9.55
15	PRB931_06.TC3.4930	1B	B	0.4	0.05
16	6244_13.B5.4576	2	B	9.4	0.9
17	6240_08.TA5.4622	2	B	2.1	0.2
18	63358.p3.4013	2	B	>10	0.3
19	THRO	2	B	>10	>10
20	PRB958_06.TB1.4305	2	B	3.1	0.35
21	SC45.4B5.2631	2	B	>10	0.25
22	WEAUd15.410.5017	2	B	3.05	0.2
23	REJO	2	B	>10	>10
24	ZM197	1B	C (African)	>10	>10
25	ZM214	2	C (African)	>10	>10
26	ZM233	2	C (African)	1	0.07
27	ZM53	2	C (African)	>10	>10
28	ZM109	1B	C (African)	>10	>10
29	ZM249	2	C (African)	>10	>10
30	QC406 envF3	2	C (African)	0.55	0.01
31	CAP45	2	C (African)	>10	>10
32	CAP210	2	C (African)	>10	>10
33	Du156	2	C (African)	0.15	0.25
34	Du172	2	C (African)	1.93	1.18
35	Du422.1	2	C (African)	1.21	0.41
36	MJ412	2	C (African)	0.031	0.054
37	16055	2	C (Indian)	>10	>10
38	25710	1	C (Indian)	1.2	0.7
39	25711	1B	C (Indian)	0.033	0.086
40	25925	1B	C (Indian)	0.107	0.04
41	26191	2	C (Indian)	>10	4.75
42	836	1A	C (Indian)	>10	0.01
43	16936	2	C (Indian)	1.4	5.55
44	70606F	ND	C (Indian)	>10	3
45	70607Z	ND	C (Indian)	>10	3.8
46	70607B	ND	C (Indian)	>10	0.6
47	70606B	ND	C (Indian)	9.95	0.9
48	70604B	ND	C (Indian)	9.93	0.75
49	70607C	ND	C (Indian)	>10	1.2
50	70406	ND	C (Indian)	>10	3.4
51	70408	ND	C (Indian)	>10	3.25
52	70402	ND	C (Indian)	>10	1.65
53	709316B	ND	C (Indian)	>10	3.3
54	UZ12A	ND	C (Indian)	>10	1.55
55	329.14.B1	2	C (Indian)	0.035	0.03
56	330.16.E6	2	C (Indian)	0.163	0.078
57	MK184	2	CD	0.79	0.04
58	BK184	2	CD	0.05	0.02
GMT				0.74	0.36
Breadth				46.50%	79.30%

IC50 Color code (ug/ml)
< 1
1-4
5-10
>10

Figure 2: Matured AIIMS-P01 lineage antibody 44m showed broad HIV-1 neutralization with improved potency. (A) Heat map depicting IC_{50} values of the matured 44m mAb tested against HIV-1 global panel. **(B)** Heat map depicting IC50 values of the 44m tested against heterologous panel of HIV-1 viruses, using a TZM-bl based neutralization assay (n=58).

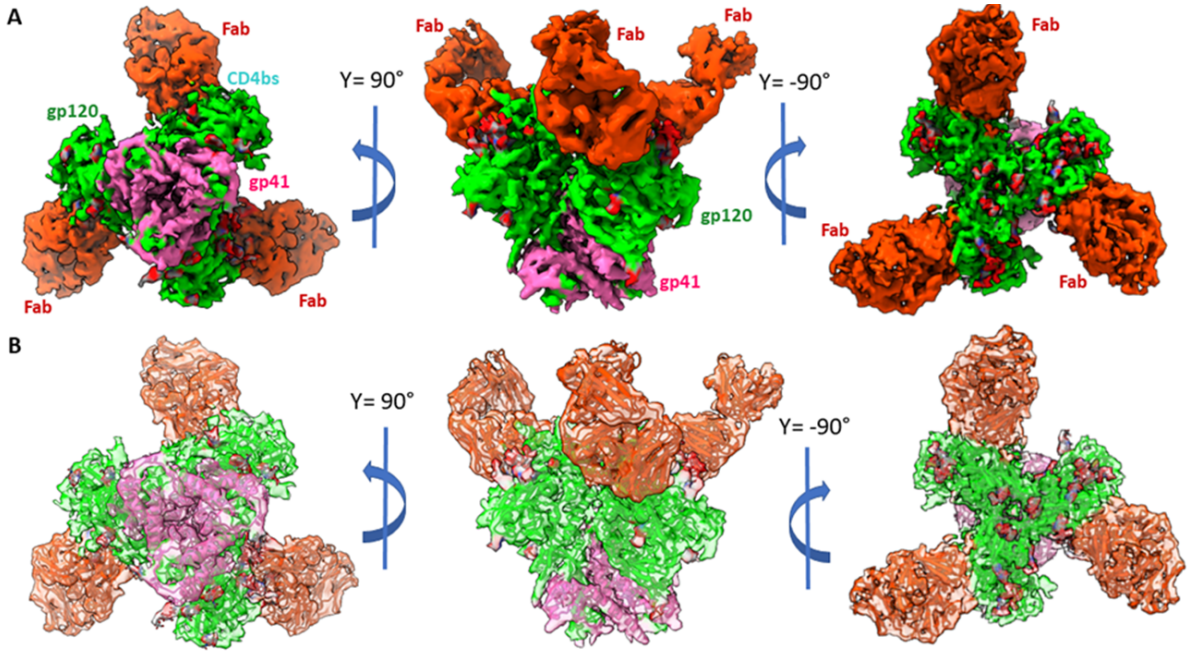

Figure 3: Cryo-EM reconstruction and model of BG505.SOSIP trimer in complex with 44m bnAb. (A) Side and top views of Cryo-EM reconstructed map of BG505.SOSIP trimer in complex with 44m bnAb solved at ~4.4Å resolution, with a local resolution in between 3.36 and 3.74Å. Color coding corresponding to segmented EM densities are: orange red, 44m bnAb; lime green, gp120; pink, gp41. **(B)** The corresponding atomic model fitted in the EM map of BG505 trimer in complex with 44m bnAb showing three 44m bnAb binds to each gp120 monomeric subunit for effective neutralization.

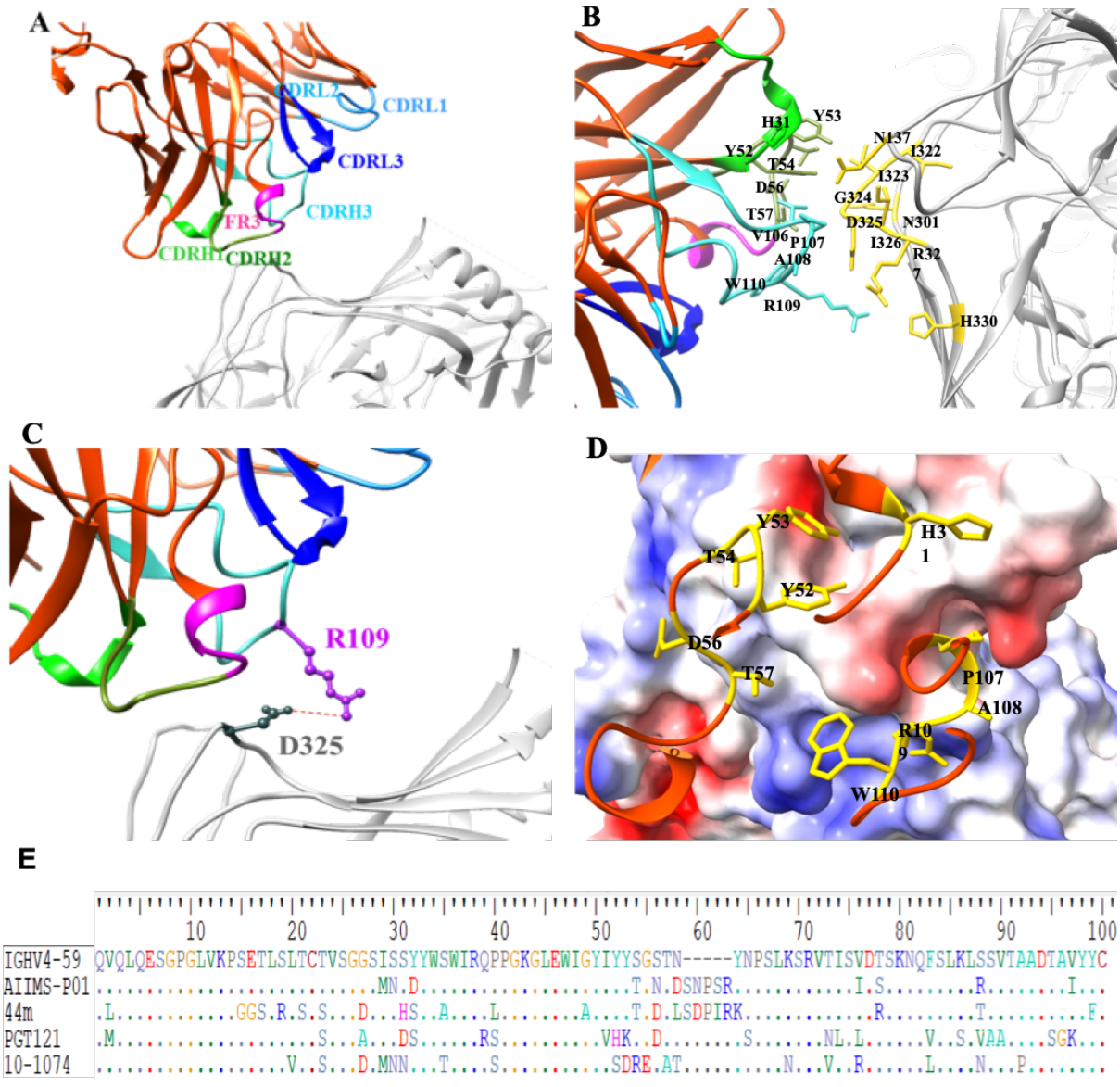

609

610 **Figure 4: Interaction sites for 44m bnAb to form a complex with BG505 SOSIP**
611 **trimer. (A)** The CDR regions in the interface of gp120 and 44m bnAb are highlighted
612 using color coding: magenta, FR3; green, CDRH1, olive green, CDRH2; and, cyan, CDRH3;
613 dodger blue, CDRL1; deep sky blue, CDRL2; median blue, CDRL3. **(B)** Salt bridge
614 interaction in between D325 residue in the V loop of gp120 monomer and CDRH1 region,
615 where D325 is shown in dark green and R109 is shown in purple color, and the bond is
616 shown in red color. **(C)** Different interacting partners in the epitope region to adapt a
617 stable conformational state with the CDR regions. **(D)** Electrostatic potential surface map
618 of the interacting region of gp120 showing the interacting residues of the paratope facing
619 towards the charged residues of the epitope. The residues on 44m bnAb is shown in
620 golden color. **(E)** Heavy chain sequence alignment of 44m bnAb with other V3-glycan
621 bnAbs belong to IGHV4-59 gene.

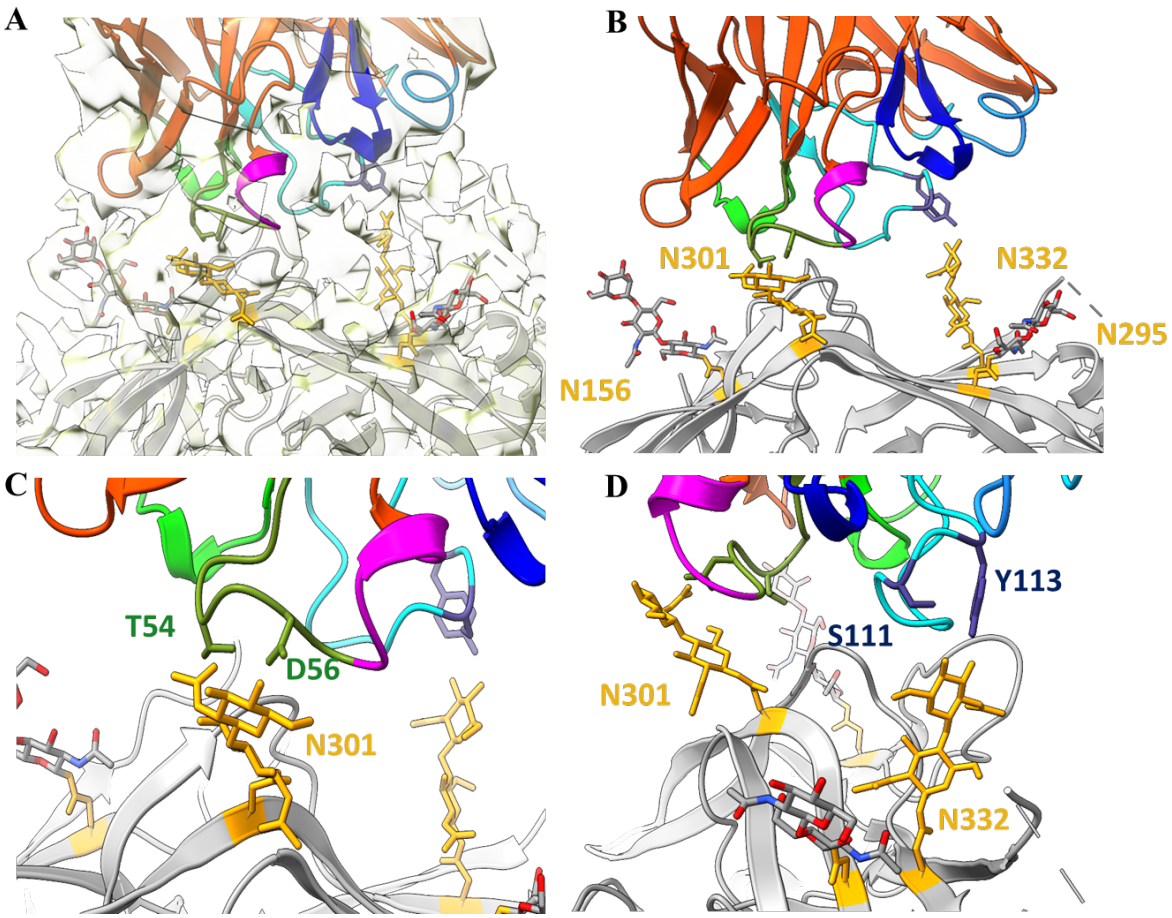

Figure 5: Glycan interaction sites of BG505.SOSIP trimer in complex with 44m Fab. **(A)** Positions and fitting different glycan residues are pointed in the EM map shown. In the atomic model N301 and N332 glycans are shown in orange color, whereas the Fab and CDR regions are colored similarly to Figure 2. **(B)** The gp120 monomer is shown in gray. Atomic model illustrating various glycan residues interacting with different region of CDR regions of 44m bnAb, where glycan attached to N156 is coming closer to CDRH1 region. **(C)** The NAG attached to Asn301 is making contact points with Thr54 and Asp56 in the CDRH2 region (shown in olive drab color). **(D)** Glycan binding to Asn332 is interacting with Ser111 and Tyr113 residues of the CDRH3 region (shown in deep blue color).